

## Percolative, self-affine, and faceted domain growth in random three-dimensional magnets

Hong Ji\* and Mark O. Robbins

*Department of Physics and Astronomy, Johns Hopkins University, Baltimore, Maryland 21218*

(Received 27 April 1992)

We study the advance of an interface separating two magnetic domains in a three-dimensional random-field Ising model. An external magnetic field causes one domain to grow. Three types of growth are found. When disorder in the medium is large, the interface forms a self-similar pattern with large scale structure characteristic of percolation. As the disorder decreases, there is a critical transition to compact growth with a self-affine interface. Finally, for sufficiently weak disorder, simple faceted growth occurs. The transitions between these growth morphologies are related to results for bootstrap percolation. In the self-similar and self-affine growth regimes there are also critical transitions at the onset of steady-state motion. These are studied numerically, and found to lie in different universality classes. The critical exponents obtained from our simulations obey general scaling relations derived in the context of fluid invasion.

### I. INTRODUCTION

A variety of important physical processes involves driven motion of an interface through a disordered medium. Examples include magnetic domain-wall motion,<sup>1-4</sup> fluid invasion of porous media,<sup>5-17</sup> and spreading on heterogeneous surfaces.<sup>18</sup> In each case the disorder is time independent or quenched. This leads to very different behavior than time-varying random forces.<sup>19-23</sup> Studies of two-dimensional (2D) systems have revealed a wide range of interface morphologies and critical transitions as the relative magnitudes of the driving force, the disorder, and the local surface tension energies are varied.<sup>3,4,10,14-16</sup> These results are briefly reviewed below. We then present a study of such transitions in a three-dimensional model—magnetic domain-wall motion in the random-field Ising model on a cubic lattice.

Much progress has been made in experimental and theoretical studies of fluid invasion of 2D porous media.<sup>5-17</sup> In this process, a preexisting fluid in the porous medium is displaced by an invading fluid, which is driven by an applied pressure  $P$ . The interface between the two fluids is pinned at pressures below a value  $P_c$ , and advances continuously at higher pressures. The onset of motion is a critical transition, and scaling relations have been derived between many of the associated exponents.<sup>15,16</sup> The results fall into different universality classes depending on the effective strength of the disorder. There is a direct correspondence between these universality classes and the structure of the marginally stable interfaces at  $P_c$ . Self-similar, self-affine, and faceted structures have been found.<sup>3,4,14,15</sup>

The effective strength of the disorder depends on both the magnitude of fluctuations in the pore geometry and on the wetting properties of the invading fluid.<sup>7,8,10-16</sup> When the invading fluid wets the porous medium less

well than the displaced fluid (nonwetting invasion), adjacent segments of the interface are uncoupled and advance independently. Growth is well-described by the invasion percolation model,<sup>6</sup> which maps the problem of penetrating the most easily invaded regions of the pore space on to bond percolation. Cooperative invasion by neighboring segments of the interface becomes important as the invading fluid becomes more wetting, and the invasion percolation model breaks down.<sup>7,8,14</sup> Theoretical studies of model porous media constructed from disks with random radii indicate that there is a critical transition from the self-similar fractal growth characteristic of percolation to a smoother structure.<sup>14,15</sup> If the distribution of disk radii is narrow, lattice anisotropy is important and the interface becomes faceted.<sup>14</sup> If the geometrical disorder is large enough to suppress lattice anisotropy, the interface is a self-affine fractal with a roughness exponent  $\alpha \approx 0.8$ .<sup>14,15</sup> Several independent experiments have found similar values of  $\alpha$ ,<sup>11-13</sup> and confirmed the sharp change in growth morphology with wetting properties.<sup>7,8,10</sup>

The discovery of a system with  $\alpha = 0.8$  provoked a great deal of interest because most models for interface growth in 2D give a universal exponent of  $\alpha = 0.5$ .<sup>19-23</sup> However, all of these models assume time-varying disorder. Martys *et al.* have suggested that the increase in  $\alpha$  is associated with the critical state at the onset of motion.<sup>15</sup> This state only occurs in systems with quenched disorder, and work in progress confirms that the roughness exponent is only equal to 0.8 at  $P_c$ .<sup>24</sup> At higher pressures, the roughness exponent crosses over to 0.5 at large length scales. A similar crossover from self-similar to self-affine growth with  $\alpha = 0.5$  occurs in percolating systems.<sup>24</sup>

The physics of domain-wall motion in Ising ferromagnets is very similar to that of fluid invasion.<sup>2-4</sup> In this case, an interface separates regions of up and down spins. Growth of one domain is driven by an external mag-

netic field  $H$ , and disorder comes from local variations in the exchange coupling (random bonds) or magnetic field (random fields). Both types of disorder have been considered in recent studies of domain growth on 2D lattices.<sup>3,4</sup> As in fluid invasion, fractal percolative growth is found for strong disorder. In this limit, the state of each spin is independent of its neighbors. As the degree of disorder decreases, advance of neighboring sections of the interface becomes increasingly correlated. There is a direct transition from percolative to faceted growth in all cases studied.<sup>3,4,25</sup> Subtle differences between the growth rules for magnetic domains and fluid invasion suppress the self-affine regime found in fluid invasion.<sup>15,16</sup> In particular, there is no way to decrease the degree of lattice anisotropy without increasing the strength of the disorder. The absence of a self-affine phase in the 2D random-field Ising model appears to be related to the fact that arbitrarily weak disorder suppresses ferromagnetism.<sup>26</sup> Ferromagnetism and disorder can coexist in higher dimensions, thus one might expect a richer nonequilibrium phase diagram. This is confirmed by the data presented below.

Previous work on magnetic domain-wall motion in three and higher dimensions has focused on a continuum model which assumes that the interface is a single-valued function of position.<sup>1,2</sup> This is an important simplification because self-similar percolating domains necessarily have multivalued interfaces. Only faceted or self-affine interfaces can be treated in this model.

Bruinsma and Aeppli<sup>1</sup> applied scaling arguments to the continuum model, and concluded that disorder could pin the interface in less than five dimensions ( $H_c > 0$ ). Koplik and Levine<sup>2</sup> studied the model numerically, and reached different conclusions. In particular, they found no pinning in dimensions greater than three. Neither of these works considered the possibility of a critical transition at the onset of interface motion, or studied the morphology of the advancing interfaces.

More recently Kessler *et al.* have looked at interface roughness in a 2D version of the continuum model.<sup>23</sup> They found that the large scale structure of moving interfaces was always self-affine with  $\alpha = 0.5$ . However, their results could be fit to an apparent  $\alpha$  near 0.75 at small length scales and velocities. Kessler *et al.* argued that this value resulted from a crossover between fractal percolation behavior at small length scales ( $\alpha = 1$ ) and the large scale exponent of 0.5. They suggested that a similar crossover might produce an *apparent* exponent of 0.8 in fluid invasion at finite velocity. This view contrasts with that of Martys *et al.* who found a well-defined *intrinsic* exponent of  $\alpha = 0.81(5)$  at large length scales in the limit of zero velocity.<sup>15</sup>

In this paper, we consider magnetic domain-wall motion in 3D. As in 2D, there are faceted and percolative growth regimes at low and high disorder, respectively. There is an additional self-affine growth regime at intermediate disorder which is like that found in 2D fluid invasion. As there, the roughness exponent is much larger than the exponent for continuum models with time-varying noise.<sup>19</sup> The value of the exponent is an intrinsic property of the marginal interface at  $H_c$ . Several

other parallels to fluid invasion are found. The transition from percolation to self-affine growth is characterized by the divergence of a coherence length, or fingerwidth.<sup>14</sup> The critical behavior at the onset of motion depends only on the morphology of the marginal interface. Self-similar growth is well described by 3D percolation exponents and self-affine growth belongs to a new universality class. The critical exponents for each case are obtained numerically and tested against scaling relations derived in Ref. 16.

The paper is organized as follows. In the next section we describe the random-field Ising model and our growth algorithm. Section III contains a discussion of the changes in growth morphology as the strength of disorder varies. These changes, and the values of  $H_c$ , are related to results from bootstrap percolation theory.<sup>27</sup> The critical transitions at the onset of interface motion are analyzed in Sec. IV, and the final section presents a summary and conclusions.

## II. RANDOM-FIELD ISING MODEL AND GROWTH ALGORITHM

The Hamiltonian describing the random-field Ising model is<sup>26</sup>

$$\mathcal{H} = - \sum_{\langle ij \rangle} s_i s_j - \sum_i (H + h_i) s_i, \quad (1)$$

where the Ising spins on sites  $i$  can have values  $s_i = \pm 1$ , the first sum is over all nearest-neighbor pairs,  $H$  is the external magnetic field, and  $h_i$  represents the random local field. For convenience, we have set the exchange constant to unity and will assume the lattice constant also equals one. The probability of finding a given local field,  $h$ , at a site is given by a distribution function  $P(h)$ . The strength of disorder is characterized by the range of the distribution. Throughout this paper, we use a uniform distribution between  $-\Delta$  and  $\Delta$ . Other distributions have been studied in 2D and yield similar results.<sup>4</sup>

We consider zero-temperature single-spin-flip dynamics of Ising spins on a cubic lattice.<sup>28</sup> Since only pores on the interface can be invaded in the fluid invasion problem, we only allow spins on the interface to flip. In a true magnetic system, spin flips can occur anywhere in the system. However, as discussed in Ref. 3, we do not expect this to lead to substantial changes in the large scale structure of the growth pattern.

The growth of the interface is simulated in the following way.<sup>3</sup> We start from an initial interface between up and down spins. This interface is chosen to be a flat horizontal plane at the bottom of a simple cubic lattice containing  $L \times L \times L$  spins. Up spins are below this plane and down spins are above. Periodic boundary conditions are imposed along the horizontal directions. Down spins on the interface are flipped only if this lowers the total energy. Since  $T = 0$ , flipped spins will never flip back to the down orientation.

We begin by setting  $H$  equal to the value where the first down spin on the initial interface will flip up. This spin is flipped, which changes the exchange force on

neighboring spins. If any of these become unstable, they are also flipped. When two or more spins are unstable, the most unstable spin is flipped first. Growth stops when all spins on the interface are stable at the given  $H$ . The value of  $H$  is then increased to the value where the first spin on the new interface becomes unstable and the process is repeated. The number of spins which flip following each increase in  $H$  is stored as a measure of the degree of correlation between spin flips. Growth continues in this way until the pattern of flipped spins spans the system. The value of  $H$  required to span the system approaches a constant critical field,  $H_c$ , as the system size increases.

### III. TRANSITIONS IN GROWTH MORPHOLOGY

For systems with zero disorder ( $\Delta = 0$ ), the exchange coupling causes the interface to remain flat throughout its motion. Thus growth always yields a faceted pattern. In the opposite limit of strong disorder ( $\Delta \gg 1$ ), spin flips become independent of each other and domain growth reduces to an invasion percolation process.<sup>3,4,29</sup> Previous studies of domain growth in 2D have shown that there is a direct transition from percolative to faceted growth at  $\Delta = 1$  on the square and hexagonal lattices. On the honeycomb lattice the transition is depressed to  $\Delta = 0$ .

Figure 1 shows that the phase diagram of 3D systems is much richer. The critical external field  $H_c$  is plotted against the degree of disorder  $\Delta$ . Values of  $H_c$  were obtained by extrapolating  $H_c(L)$ , the mean value of  $H$  required to span systems of edge  $L$ , to infinite system size. Two cusps in  $H_c$  are evident at  $\Delta_1^c = 2.42$  and  $\Delta_2^c = 3.41$ . As illustrated in Fig. 2, these cusps separate the three types of growth morphology. Cross sections of stable domains in  $L = 100$  systems are shown at the highest field before the flipped spins spanned the entire system. Dark regions represent flipped spins. Isolated islands of flipped spins come from overhangs. They are connected to the domain through the dimension perpendicular to the cross section.

For systems with weak disorder ( $\Delta < \Delta_1^c$ ), growth yields faceted patterns [Fig. 2(a)]. In this regime, the exchange coupling between neighboring spins dominates

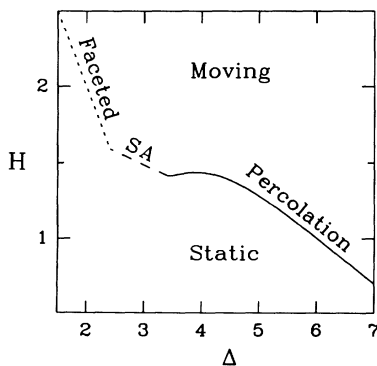


FIG. 1. Variation of  $H_c$  with  $\Delta$ . Cusps occur at  $\Delta_1^c = 2.42$  and  $\Delta_2^c = 3.41$ . The self-affine growth regime is indicated by "SA".

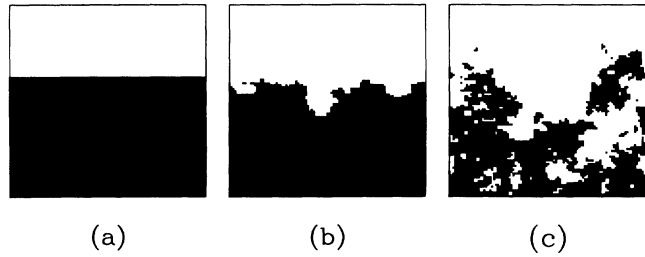


FIG. 2. Vertical cross sections of the domain structure for (a)  $\Delta = 2$ , (b)  $\Delta = 3$ , and (c)  $\Delta = 4.4$ . Dark regions represent flipped spins, and growth was started from a flat interface at the bottom of the cubic lattice.

the growth process. As discussed below, an entire plane of spins adjacent to the interface can flip as soon as one spin on the interface becomes unstable.<sup>3</sup> Thus the growing interface remains flat.

For intermediate disorder,  $\Delta_1^c < \Delta < \Delta_2^c$ , the domain walls are self-affine fractals [Fig. 2(b)]. Self-similar fractals such as percolation clusters are isotropic and are scale invariant when magnified equally in all directions.<sup>5</sup> In contrast, a self-affine fractal is anisotropic.<sup>5</sup> Different scaling factors are required in the longitudinal and transverse directions, and at large scales the interface appears flat. The degree of anisotropy is described by the roughness exponent  $\alpha$  which is the logarithmic ratio of the transverse and longitudinal scaling factors. One way of determining  $\alpha$  is shown in Fig. 3. The rms fluctuation of the interface height,  $\delta h$ , is calculated over horizontal regions of width  $\delta x$ . Self-affinity implies a power law relation:  $\delta h \sim \delta x^\alpha$ . Figure 3 shows  $\log_{10}(\delta h)$  vs  $\log_{10}(\delta x)$  for  $\Delta = 2.8$  and system size  $L = 300$ . Values of  $\delta h$  were calculated for the last stable interface before the domain spanned a system. They were then averaged over all regions of width  $\delta x$  and different configurations of random fields. Results for  $L = 50$  and 100 were analyzed to

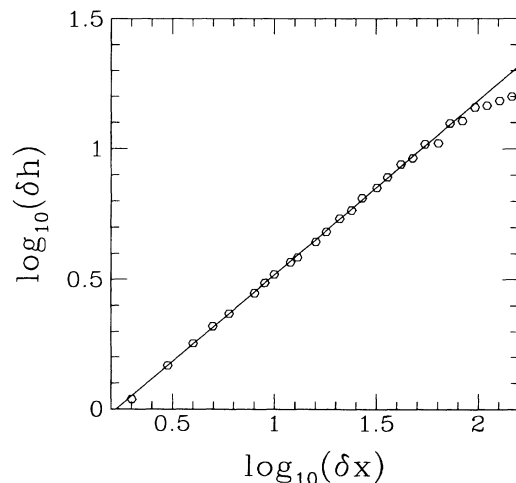


FIG. 3. Variation of  $\delta h$  with  $\delta x$  for  $\Delta = 2.8$  in systems with  $L = 300$ . The slope of the linear fit is  $\frac{2}{3}$ .

check for finite-size effects. From the slope of these plots we found  $\alpha = 0.67(3)$ . We have also determined  $\alpha$  for  $\Delta = 2.6$  and  $3.0$ , and obtained the same value within the quoted error bars.

Our result for  $\alpha$  is substantially larger than the roughness exponent  $\alpha = 0.4$  obtained<sup>21,22</sup> from the Kardar-Parisi-Zhang (KPZ) equation<sup>19</sup> for surface growth. The KPZ equation describes models where the disorder is annealed, i.e., the random force on a site averages to zero over time. Our random fields are independent of time so that fluctuations can not average out. As in 2D fluid invasion,<sup>11–15</sup> this produces a rougher interface.

The calculated roughness exponent agrees well with the prediction of scaling theory for the conformation of the lowest energy interface in a random-field Ising model.<sup>26</sup> Comparing the energy gain due to interactions with the random field, to the energy cost of increased interfacial area, one finds an optimal size  $\delta h$  for deformations over interface regions of size  $\delta x$ . The associated roughness exponent is  $\alpha = (5 - d)/3$ , where  $d$  is the spatial dimension of the medium.<sup>26</sup> It is interesting that an external field drives the system to a final stable configuration which has the same scaling properties. While this final state has the maximum pinning force, it need not minimize the energy. Note that the above expression gives  $\alpha = 1$  in 2D. This corresponds to isotropic, self-similar scaling, and is consistent with the fact that no self-affine growth regime is observed for 2D magnetic domains.<sup>3,4</sup>

Figure 2(c) shows the typical growth morphology in systems with strong disorder ( $\Delta > \Delta_2^c$ ). The domain exhibits the intricate self-similar structure characteristic of 3D percolation clusters.<sup>30,31</sup> To quantify the comparison we have calculated the fractal dimension of domains,  $D_f$ , using the box counting method.<sup>5</sup> Patterns used to calculate the fractal dimension were obtained by terminating growth when a stable interface spanned the system. Results were averaged over at least 20 different configurations of random fields at  $\Delta = 6$ . Several different system sizes were used ( $L = 64, 128, 256$ ) to check for finite-size effects. We found that growth patterns were self-similar and that the fractal dimension was  $D_f = 2.5(1)$ . This value is consistent with the fractal dimension of ordinary 3D percolation.<sup>30,31</sup>

The large scale structure for other values of  $\Delta > \Delta_2^c$  is characterized by the same fractal dimension. However, the patterns become markedly coarser at short scales as  $\Delta$  decreases. This coarsening reflects coherent flipping of larger and larger regions of neighboring spins. To quantify the increasing range of correlations, we introduce a mean fingerwidth  $w$ . This quantity is obtained by making parallel lines slicing through the system, and calculating the mean length of the segments which lie inside the domain of flipped spins. The same measure has been used in our 2D simulations,<sup>3,4</sup> as well as in experimental<sup>8,10</sup> and theoretical<sup>14–17</sup> studies of fluid invasion.

Figure 4 shows the fingerwidth as a function of  $\Delta$  for three different system sizes. For large  $\Delta$ ,  $w$  is small (a few lattice constants) and independent of system size. As  $\Delta$  decreases,  $w$  increases and the growth pattern coarsens. However, the structure remains self-similar at

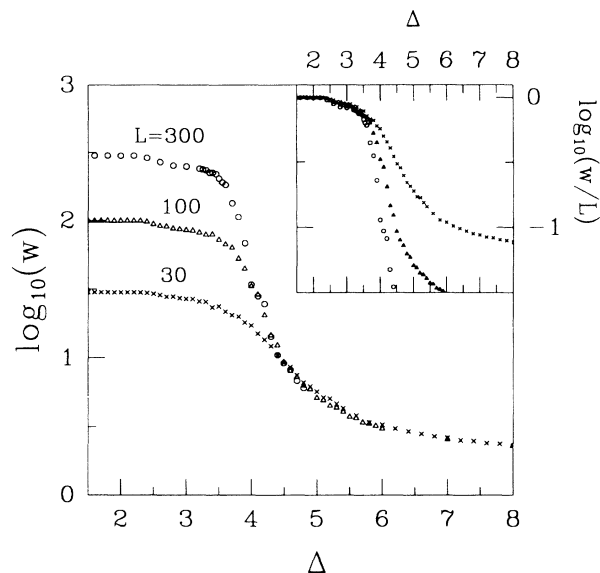


FIG. 4. Fingerwidth  $w$  vs  $\Delta$  for the indicated system sizes  $L$ . Note that  $w$  saturates at  $L$  for  $\Delta < \Delta_1^c$ . The inset shows  $w/L$  vs  $\Delta$ . It is independent of  $L$  for  $\Delta < \Delta_2^c$ .

scales larger than  $w$ , with the same fractal dimension. As  $\Delta$  approaches the critical point  $\Delta_2^c = 3.41$  from above,  $w$  would diverge in an infinite system. This signals a transition from percolation to self-affine growth. Similar divergences are observed at the transition from percolation to faceted growth in 2D magnetic systems<sup>3,4</sup> and at the transition from percolation to self-affine growth in 2D fluid invasion.<sup>14,15</sup>

The divergence of  $w$  is most clearly seen from the inset of Fig. 4 where  $w/L$  is plotted against  $\Delta$ . For  $\Delta < \Delta_1^c$ , the fingerwidth always equals the system size ( $w/L = 1$ ) and growth is faceted. For  $\Delta \leq \Delta_2^c$ , results for different system sizes collapse onto a universal curve. Thus  $w$  scales with  $L$  and would diverge in an infinite system ( $L \rightarrow \infty$ ). Based on our 2D studies<sup>4</sup> we expect  $w$  to diverge as a power law,  $w \propto (\Delta - \Delta_2^c)^{-\nu'}$ . We have determined the exponent  $\nu'$  using a finite-size scaling ansatz<sup>3,4</sup>

$$w(L) = Lf[L^{1/\nu'}(\Delta - \Delta_2^c)/\Delta]. \quad (2)$$

As in 2D,<sup>4</sup> the scaling variable  $(\Delta - \Delta_2^c)/\Delta$  gives better fits than  $(\Delta - \Delta_2^c)/\Delta_2^c$ . Best fits to data from  $L = 30$  to 300 give  $\nu' = 3.0(5)$ . The large error bars reflect substantial corrections to finite-size scaling that appear for either scaling variable. Our 2D studies show that  $\nu'$  is not universal, but depends on the analytic form of the edges of the distribution of random fields.<sup>4</sup> The same arguments apply here.

The changes in growth morphology with disorder are closely related to variations in the probabilities that spins with different local environments will flip. In the Ising model this probability only depends on  $H$ ,  $P(h)$ , and the number  $n$  of neighboring spins which have flipped. The fraction of spins which would flip at  $H_c$  if they had  $n$  flipped neighbors is given by

$$f_n = \int_{-\infty}^{H_c} P(z - 2n - H) dH = (H_c - z + 2n + \Delta)/2\Delta, \quad (3)$$

where  $z = 6$  is the coordination number of the cubic lattice and the last equality only holds for a uniform distribution of local fields. The calculated variation of  $f_n$  with  $\Delta$  is shown in Fig. 5. Note that  $f_1$  becomes non-zero at the transition from faceted to self-affine growth ( $\Delta_1^c$ ) and  $f_4$  becomes less than unity at the transition to percolation ( $\Delta_2^c$ ).

As in 2D,<sup>4</sup> these transitions can be better understood by using an analogy between domain growth and bootstrap or diffusion percolation.<sup>27</sup> In bootstrap percolation lattice sites are occupied randomly with probability  $p$ . Then all sites which do not have at least  $m$  occupied neighbors are removed. In the corresponding diffusion percolation problem, unoccupied sites with at least  $z - m + 1$  occupied neighbors are *occupied*. The percolation probability  $p_c$  is defined as the minimum probability required for the final set of occupied sites to span the system. The magnetic domain growth problem corresponds<sup>4</sup> to a continuous generalization of such models in which the probabilities of occupation are not unity, but are instead given by  $f_n$ .

The value of  $H_c$  in the faceted regime can be obtained from results for diffusion percolation on a square lattice. The initial interface is a square lattice at the bottom of the system. Interface spins have  $n = 1$  flipped spin and 5 unflipped spins as neighbors. The lowest field at which a spin can flip is thus  $H_1^* = 4 - \Delta$ . At any field greater than  $H_1^*$  there will be a finite fraction of flipped spins on the interface. Studies of diffusion percolation on the square lattice show that  $p_c = 0$  if all sites with two occupied neighbors become occupied. In our system, spins with two flipped neighbors on the planar interface would have a third flipped neighbor in the plane below, giving  $n = 3$ . All such spins would flip by  $H_3^* = \Delta$ , since the net exchange interaction is zero for  $n = 3$ . Thus bootstrap percolation tells us that as long as  $H_1^* > H_3^*$  the entire interface will flip at  $H_1^*$ . This implies

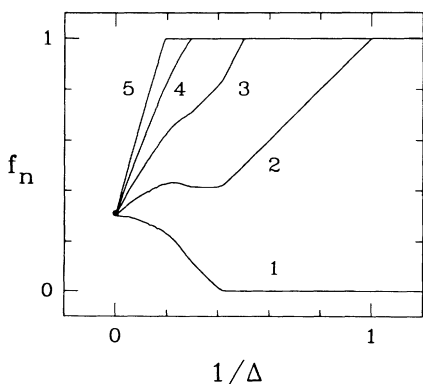


FIG. 5. Probabilities that spins with  $n$  flipped neighbors will flip at  $H_c$  as a function of  $1/\Delta$  for the indicated values of  $n$ .

$$H_c = 4 - \Delta \quad (4)$$

in the faceted regime. The faceted regime actually extends beyond the regime where  $H_1^* > H_3^*$  (i.e.,  $\Delta < 2$ ). The reason is that there is a substantial probability ( $f_2 > 0.4$ ) that spins with only two neighbors will flip. In diffusion percolation this probability would be zero and percolation would be more difficult.

Figure 5 shows that  $f_4 = 1$  in the self-affine regime, and that  $f_2 = (f_1 + f_3)/2$  has a constant value of 0.4138(5). Two previous numerical studies give values of  $p_c = 0.4283(5)$  and 0.432(20) for diffusion percolation on the cubic lattice with sites with four neighbors occupied.<sup>27</sup> These values are very close to our value of  $f_2$  in the self-affine regime. They need not be identical since the domain growth model does not begin by flipping a randomly chosen set of spins to the up position. Using a best fit value to  $f_2$  in the self-affine regime we find

$$H_c = 2 - (1 - 2f_2)\Delta = 2 - 0.1724\Delta. \quad (5)$$

The intersection between this line and Eq. (4) gives our best determination of the location of the transition to faceted growth,  $\Delta_1^c = 1/f_2 = 2.417(4)$ . The intersection of this line with the line where  $f_4$  begins to differ from 1 gives our best estimate of the transition to percolation  $\Delta_2^c = 2/(1 - f_2) = 3.412(5)$ .

In the limit of very large  $\Delta$ , the exchange coupling is irrelevant and all of the  $f_n$  converge to a common value. As shown in Fig. 5 this is consistent with the normal percolation probability on the cubic lattice,  $p_c = 0.3117$ . An exact bound on  $H_c$  can be obtained by noting that  $f_n > f_1$  for  $n > 1$ . Then if  $f_1 = p_c$  all other  $f_n$ 's are higher and the pattern must percolate. (Note that isolated sites,  $n = 0$ , are irrelevant.) Thus from Eq. (3)

$$H_c < (2p_c - 1)\Delta + 4 = 4 - 0.3766\Delta. \quad (6)$$

In the limit of large  $\Delta$ , the exact  $H_c$  becomes parallel to this line.

#### IV. CRITICAL ONSET OF DOMAIN-WALL MOTION

In the previous section, we studied changes in growth morphology with the strength of disorder. In this section, we consider the critical transitions which occur as  $H$  increases to  $H_c$  in the percolation and self-affine regimes. The faceted regime does not exhibit an analogous critical transition because there is a finite range of  $H$  between  $H_3^* = \Delta$  and  $H_c = H_1^*$  where the only stable interfaces are (100) planes of the cubic lattice. There is no growth in this regime and the entire lattice is filled as soon as  $H = H_c$ .

The idea that the onset of motion in a disordered system could be a critical transition was advanced by Fisher<sup>32</sup> in the context of charge-density wave (CDW) conductors. The basic argument is readily extended to magnetic domain growth. If the spatial dimension is sufficiently low, the domain wall will be distorted by the random field until it reaches a local energy minimum. At

zero external magnetic field, there will be a rich hierarchy of metastable states. The interface will initially be “pinned” in one local minimum. As the magnetic field increases, that minimum may become unstable, allowing the interface to advance to the nearest metastable state. The number of metastable states decreases with increasing magnetic field, so that larger rearrangements of the interface are needed to reach a new metastable state. It is natural to associate the scale of rearrangements with a diverging coherence length. At a critical magnetic field  $H_c$ , the last state becomes unstable and the entire system evolves coherently.<sup>15</sup>

Martys, Robbins, and Cieplak<sup>16</sup> have identified several quantities which describe the critical behavior as  $H$  approaches  $H_c$  from below. Two are the total volume of the domain,  $V_t$ , and the total external surface area,  $S_e$ . A third is the mean volume,  $\langle V \rangle$ , of the incremental growths which follow each increase in  $H$ . All of these quantities show power law divergences at  $H_c$ :

$$\begin{aligned} V_t &\propto L^{d-1}(H_c - H)^{-\psi}, \\ S_e &\propto L^{d-1}(H_c - H)^{-\omega}, \\ \langle V \rangle &\propto (H_c - H)^{-\phi}, \end{aligned} \quad (7)$$

where the powers of  $L$  indicate the scaling with the size of the initial interface.<sup>16</sup> Such divergences typically reflect power law correlations at the critical point. In our case, these correlations produce a power law distribution in the size of incremental growths at  $H_c$ :

$$\rho(V) \propto V^{-\tau'}. \quad (8)$$

As shown in Ref. 16, these and other exponents can be related by scaling laws similar to those obeyed at equilibrium critical transitions. Only three exponents are needed to determine all others. These are most conveniently chosen to be the bulk and external fractal dimensions,  $D_f$  and  $D_e$ , and the correlation length exponent  $\nu$ :

$$\xi \propto (H_c - H)^{-\nu}. \quad (9)$$

General expressions<sup>16</sup> for the scaling laws are given in the first column of Table I. Subsequent columns give simplified forms valid for the cases of interest here. In the self-affine regime we use the fact that  $D_f = D_e + 1 = d$ . In the self-similar regime in 3D we have  $D_f = D_e$ .<sup>33</sup> Thus

TABLE I. General scaling laws obeyed by critical exponents for invasion (Ref. 16), specialized expressions for compact growth where  $D_f = D_e + 1 = d$ , and specialized forms for 3D percolation where  $D_f = D_e$ . The expression for  $\tau'$  has been obtained from independent arguments by Gouye (Ref. 34).

	General	$D_f = D_e + 1 = d$	$D_f = D_e$
$\psi$	$\nu(D_f + 1 - d)$	$\nu$	$\nu(D_f + 1 - d)$
$\omega$	$\nu(D_e + 1 - d)$	0	$\psi$
$\phi$	$1 + \nu(D_f - D_e)$	$1 + \nu$	1
$B$	$D_f - D_e + \nu^{-1}$	$1 + \nu^{-1}$	$\nu^{-1}$
$\tau'$	$1 + (D_e - \nu^{-1})D_f^{-1}$	$2 - (1 + \nu^{-1})d^{-1}$	$2 - (\nu D_f)^{-1}$

there is a single unknown exponent for self-affine growth and two unknown exponents for self-similar growth.

Numerical determination of the critical exponents is complicated by system-size induced cutoffs in critical quantities. Thus, following Ref. 16, we use a finite-size scaling ansatz and data for several different system sizes to obtain values for the exponents. The basic idea is that near the critical point,  $H_c$ , the only relevant length scales are the system size  $L$  and a correlation length  $\xi$ . Hence, appropriately normalized quantities should only depend on the ratio of  $L$  to  $\xi$ . This ratio is usually expressed in terms of a scaling parameter:  $x = L^{1/\nu}(H_c - H)/H_c$ . By examining the scaling of quantities with system size at  $H_c$  ( $x = 0$ ), one determines scaling forms for the diverging quantities:<sup>16</sup>

$$\begin{aligned} V_t(H, L) &= L^{D_f} g(x), \\ S_e(H, L) &= L^{D_e} g_S(x), \\ \langle V(H, L) \rangle &= L^B h(x), \end{aligned} \quad (10)$$

where  $g$ ,  $g_S$ , and  $h$  are universal functions, and  $B$  is given in Table I.

We have used these relations to study domain-wall motion for  $\Delta = 3$  (compact self-affine growth) and  $\Delta = 6$  (percolation-like growth). Values of  $D_f$  and  $H_c$  were obtained by using the fact that  $V_t/L^{D_f}$  is independent of system size at  $H = H_c$  ( $x = 0$ ). Thus plots of  $V_t/L^{D_f}$  versus  $H$  for different system sizes should intersect at a common point,  $H_c$ . For  $\Delta = 3$  we assumed  $D_f = 3$  and found curves for  $L = 30, 50, 100$ , and  $200$  intersected, within statistical fluctuations, in the range quoted for  $H_c$  in Table II. For  $\Delta = 6$ ,  $D_f$  was varied. The range of values for  $D_f$  and  $H_c$  over which there was a common intersection for system sizes 30–200 is also indicated in Table II. The resulting value of  $D_f$  is consistent with direct determinations using the box counting method.

TABLE II. Critical exponents from finite-size scaling fits for self-affine ( $\Delta = 3$ ) and self-similar ( $\Delta = 6$ ) growth. Error bars in the last significant digit are given in parentheses and indicate the maximum range consistent with the finite-size scaling fit. All quantities were evaluated through independent fits. For  $\Delta = 6$  the leftmost value of  $D_f$  was obtained directly from the structure and the rightmost value came from finite-size scaling fits. Within our uncertainties the exponents are consistent with the scaling laws of Table I. Exponents for self-similar growth are also consistent with those for ordinary percolation. Quoted values for 3D percolation come from Ref. 31 and error bars reflect the range of values reported from different methods. For percolation  $\psi = \nu - \beta$ .

	$\Delta = 3$	$\Delta = 6$	3D
	$H_c = 1.4797(3)$	$H_c = 1.011(2)$	perc.
$D_f$	3	2.5(1), 2.48(3)	2.53(3)
$D_e$	2	2.5(1)	2.53(3)
$\alpha$	0.67(3)		
$\nu$	0.75(5)	0.9(1)	0.88(2)
$\psi$	0.75(5)	0.47(7)	0.45(5)
$\phi$	1.71(11)	0.90(15)	1
$B$	2.2(2)	1.05(10)	1.13(3)
$\tau'$	1.28(5)	1.59(5)	1.55(2)

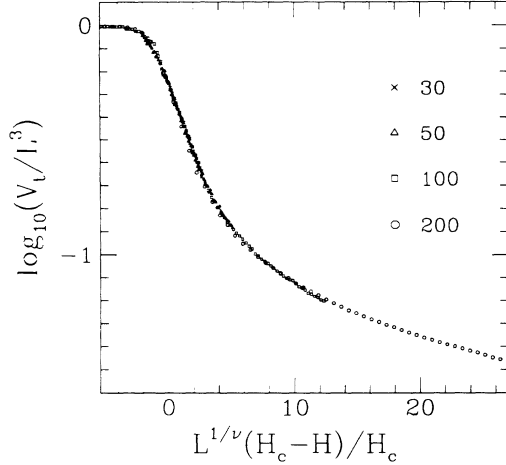


FIG. 6. Finite-size-scaling collapse of  $V_t$  at  $\Delta = 3$  with  $H_c = 1.4797$  and  $\nu = 0.78$  and the indicated system sizes.

Given values of  $H_c$ , we determined  $\psi$  and  $\phi$  directly by fitting the divergences of  $V_t$  and  $\langle V \rangle$  to power law forms. Finite-size effects were minimized by restricting the fit to regions where results for different system sizes coincided. The resulting values and uncertainties are quoted in Table II.

Values of  $\nu$  were determined using the finite-size scaling forms for  $V_t$  and  $\langle V \rangle$  in Eq. (10). Figures 6 and 7 illustrate the quality of the data collapse for  $\Delta = 3$  and 6, respectively. Only data from the scaling regime are plotted. For  $\Delta = 3$  this corresponded to  $H > 1.43$  and for  $\Delta = 6$  to  $H > 0.98$ . At smaller  $H$  there is a systematic deviation from the universal curve because  $\xi$  is comparable to the lattice constant. The range of values for  $\nu$  quoted in Table II reflects the uncertainties in  $H_c$  and, for  $\Delta = 6$ , in  $D_f$ . The same range of values fit data for  $\langle V \rangle$ . In the latter case we also allowed  $B$  to vary independently (Table II). This exponent is most susceptible to systematic uncertainties because of the small range of  $L$  studied.

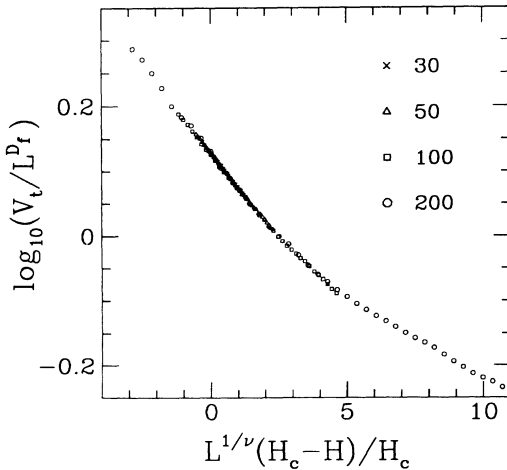


FIG. 7. Finite-size-scaling collapse of  $V_t$  at  $\Delta = 6$  with  $H_c = 1.011$ ,  $\nu = 0.90$ ,  $D_f = 2.49$ , and the indicated system sizes.

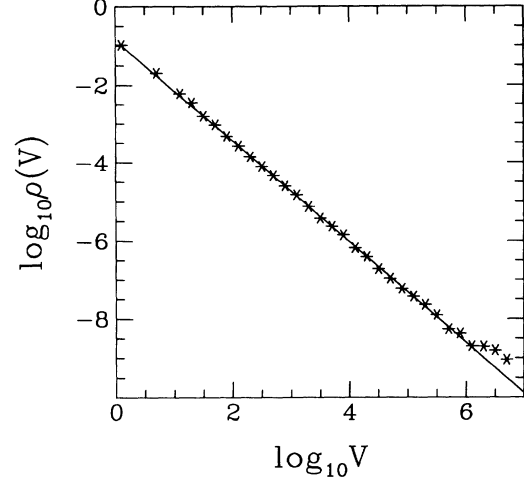


FIG. 8. Distribution of growths at  $L = 300$  for  $\Delta = 3$ . Data were averaged over the range  $|L^{1/\nu}[H_c - H]/H_c| < 1$  and the slope of the linear fit is 1.28.

Figures 8 and 9 show  $\ln \rho(V)$  versus  $\ln V$  for  $\Delta = 3$  and  $\Delta = 6$ , respectively. Data were obtained for system size  $L = 200$  in a range of fields where the distribution of growths is cut off by the system size rather than the coherence length,  $L^{1/\nu}|H - H_c|/H_c < 1$ . In both figures,  $\rho(V)$  follows a power law over nearly 6 orders of magnitude. The slopes of the plots give the values of  $\tau'$  quoted in Table II. The same values were obtained from finite-size scaling fits using the ansatz:<sup>16</sup>

$$\rho(V, L) = L^{-\tau' D_f} f(V/L_f^D). \quad (11)$$

The independently determined values of  $D_f$ ,  $\nu$ ,  $\psi$ ,  $\phi$ ,  $B$ , and  $\tau'$  provide a test of the scaling relations of Table I. It is readily verified that all results are consistent with these relations, subject to the statistical uncertainties. Note that there may be comparable or larger systematic errors in the exponents due to the restricted size of the systems studied. This may explain why the overlap of

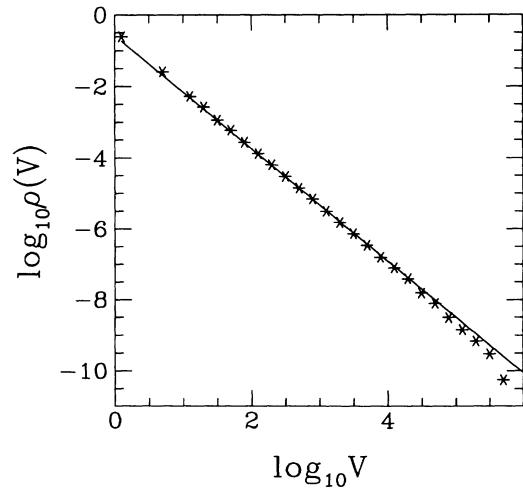


FIG. 9. Distribution of growths at  $L = 200$  for  $\Delta = 6$ . Data were averaged over the range  $|L^{1/\nu}[H_c - H]/H_c| < 1$  and the slope of the linear fit is 1.59.

the range of uncertainties is small in some cases. Note also that the results for  $\Delta = 6$  are consistent with independent determinations of critical exponents for ordinary percolation, and with values of  $\psi$ ,  $\phi$ ,  $B$ , and  $\tau'$  calculated from Table I.

## V. SUMMARY AND CONCLUSIONS

We have studied magnetic domain-wall growth in the 3D random-field Ising model. Three different growth morphologies occur, depending on the strength of the random fields,  $\Delta$ . When the disorder is large,  $\Delta > \Delta_2^c = 3.41$ , growth is percolation-like. At intermediate degrees of disorder,  $\Delta_1^c < \Delta < \Delta_2^c$ , growth is compact and the domain wall forms a self-affine fractal. For  $\Delta < \Delta_1^c = 2.42$ , growth is faceted. The self-affine regime seems to be favored by higher dimensionality. Previous studies of domain growth in the 2D random-field Ising model found a direct transition from percolation to faceted growth.<sup>3,4</sup> A self-affine regime is found in some 2D models<sup>15,16</sup> and in experiments on fluid invasion,<sup>11-13</sup> and it remains unclear what mechanisms are needed to stabilize it in 2D.

The roughness exponent for interfaces in the self-affine regime is  $\alpha = 0.67$ . This value is larger than the roughness exponent obtained from the KPZ model for interface growth,<sup>19</sup> but agrees with scaling arguments for the structure of the lowest energy state of a domain wall.<sup>26</sup> The fractal dimension of patterns in the large disorder limit is consistent with that for ordinary 3D percolation clusters (Table II). The self-similar scaling begins at length scales larger than a characteristic fingerwidth,  $w$ . This length scale diverges at the transition between self-similar and self-affine growth (Fig. 4).

The transitions between the three growth regimes were shown to correlate with changes in the probabilities that local spin configurations were stable. By mapping the problem onto a continuous family of correlated percolation problems,<sup>4,27</sup> we were able to put bounds on the critical fields in the three regimes. The random-field Ising model only spans a small subset of the space of possible

percolation models.<sup>4</sup> It remains to be seen whether still other growth morphologies may occur in other models.

For both percolation-like and self-affine growth, we studied the critical transitions at the onset of steady-state motion of the interface. The exponents obtained from the simulations clearly belong to two different universality classes. Both sets of exponents satisfy the scaling relations of Ref. 16, and results in the percolation regime are consistent with ordinary percolation. Larger systems are needed to provide more precise values for the exponents. Unfortunately, these correlated growth models require that the entire interface remain stored in memory. This prevents the application of tricks which are successful in treating normal percolation.<sup>30</sup>

There should be related critical exponents for  $H > H_c$ . For example, we expect that there is a coherence length which diverges with the exponent  $\nu$ , and that the mean velocity of the interface rises from zero as a nontrivial power of  $H - H_c$ . These expectations are born out by preliminary studies in 2D,<sup>24</sup> but 3D systems remain unexplored.

*Note added in proof.* A recent  $\epsilon$ -expansion calculation which is applicable to the self-affine regime gives exponents in agreement with our numerical values:  $\alpha = \frac{2}{3}$ ,  $\nu = \frac{3}{4}$  [T. Nattermann, S. Stepanow, L.-H. Tang, and H. Leschhorn, *J. Phys. (Paris) II* **2**, 1483 (1992)]. Additional work indicates that these results are correct to all orders in  $\epsilon$  [O. Narayan and D. S. Fisher (unpublished)].

## ACKNOWLEDGMENTS

We thank B. Koiller, C. Lobb, and N. Martys for useful discussions. Support from the National Science Foundation through Grant No. DMR-9110004 and the Donors of the Petroleum Research Foundation, administered by the American Chemical Society is gratefully acknowledged. M.O.R. also thanks the members of the Theoretical Physics Institute at the University of Minnesota for their hospitality during the period when this work was completed.

\*Current address: Physique de la Matière Condensée, Collège de France, 11, Place Marcelin-Berthelot, 75231 Paris CEDEX 05, France.

<sup>1</sup>R. Bruinsma and G. Aeppli, *Phys. Rev. Lett.* **52**, 1547 (1984).

<sup>2</sup>J. Koplik and H. Levine, *Phys. Rev. B* **32**, 280 (1985).

<sup>3</sup>H. Ji and M. O. Robbins, *Phys. Rev. A* **44**, 2538 (1991).

<sup>4</sup>B. Koiller, H. Ji, and M. O. Robbins, *Phys. Rev. B* **46**, 5258 (1992).

<sup>5</sup>See, e.g., J. Feder, *Fractals* (Plenum, New York, 1988).

<sup>6</sup>R. Lenormand and S. Bories, *C. R. Acad. Sci. Ser. B* **291**, 279 (1980); R. Chandler, J. Koplik, K. Lerman, and J. F. Willemsen, *J. Fluid Mech.* **119**, 249 (1982).

<sup>7</sup>R. Lenormand, *J. Phys.: Condens. Matter* **2**, SA79 (1990); R. Lenormand and C. Zarccone, *Phys. Rev. Lett.* **54**, 2226 (1985).

<sup>8</sup>J. P. Stokes, D. A. Weitz, J. P. Gollub, A. Dougherty, M. O. Robbins, P. M. Chaikin, and H. M. Lindsay, *Phys. Rev. Lett.* **57**, 1718 (1986).

<sup>9</sup>J. P. Stokes, A. P. Kushnick, and M. O. Robbins, *Phys. Rev. Lett.* **60**, 1386 (1988).

<sup>10</sup>A. Kushnick, J. P. Stokes, and M. O. Robbins, in *Fractal Aspects of Materials: Disordered Systems*, edited by D. A. Weitz, L. M. Sander, and B. B. Mandelbrot (Materials Research Society, Pittsburgh, 1988), pp. 87-89.

<sup>11</sup>M. A. Rubio, C. Edwards, A. Dougherty, and J. P. Gollub, *Phys. Rev. Lett.* **63**, 1685 (1989); **65**, 1339 (1990).

<sup>12</sup>V. K. Horváth, F. Family, and T. Vicsek, *Phys. Rev. Lett.* **65**, 1388 (1990); *J. Phys. A* **24**, L25 (1991).

<sup>13</sup>P.-z. Wong (private communication).

<sup>14</sup>M. Cieplak and M. O. Robbins, *Phys. Rev. Lett.* **60**, 2042 (1988); *Phys. Rev. B* **41**, 11508 (1990).

<sup>15</sup>N. Martys, M. Cieplak, and M. O. Robbins, *Phys. Rev. Lett.* **66**, 1058 (1991).

<sup>16</sup>N. Martys, M. O. Robbins, and M. Cieplak, *Phys. Rev. B* **44**, 12294 (1991).

<sup>17</sup>B. Koiller, H. Ji, and M. O. Robbins, *Phys. Rev. B* **45**, 7762 (1992).



- <sup>18</sup>M. O. Robbins and J.-F. Joanny, *Europhys. Lett.* **3**, 729 (1987).
- <sup>19</sup>M. Kardar, G. Parisi, and Y. Zhang, *Phys. Rev. Lett.* **64**, 543 (1990).
- <sup>20</sup>E. Medina, T. Hwa, M. Kardar, and Y.-C. Zhang, *Phys. Rev. A* **39**, 3053 (1989).
- <sup>21</sup>J. Amar and F. Family, *J. Phys. A* **24**, L79 (1991).
- <sup>22</sup>J. M. Kim and J. M. Kosterlitz, *Phys. Rev. Lett.* **62**, 2289 (1989).
- <sup>23</sup>D. A. Kessler, H. Levine, and Y. Tu, *Phys. Rev. A* **43**, 4551 (1991).
- <sup>24</sup>M. O. Robbins, M. Ciepak, H. Ji, B. Koiller, and N. Martys, in *Proceedings of the NATO ARW on Growth Patterns in Physical Sciences and Biology, Granada, Spain, 1991*, edited by L. Sander and P. Meakin (Plenum, New York, 1992); C. Nolle, N. Martys, B. Koiller, and M. O. Robbins (unpublished).
- <sup>25</sup>If the distribution of random fields or bonds is not bounded, this transition occurs in the limit of zero disorder.
- <sup>26</sup>G. Grinstein and S. Ma, *Phys. Rev. B* **28**, 2588 (1983).
- <sup>27</sup>J. Chalupa, P. L. Leath, and G. R. Reich, *J. Phys. C* **12**, L31 (1981); P. M. Kogut and P. L. Leath, *ibid.* **14**, 3187 (1981); J. Adler and J. Aharony, *J. Phys. A* **21**, 1387 (1988), and references therein.
- <sup>28</sup>S. Anderson and G. Mazenko, *Phys. Rev. B* **33**, 2007 (1986).
- <sup>29</sup>D. Wilkinson and J. F. Willemsen, *J. Phys. A* **16**, 3365 (1983).
- <sup>30</sup>See, for example, D. Stauffer, *Introduction to Percolation Theory* (Taylor and Francis, London, 1985).
- <sup>31</sup>J. Adler, Y. Meir, A. Aharony, and A. B. Harris, *Phys. Rev. B* **41**, 9183 (1990).
- <sup>32</sup>D. S. Fisher, *Phys. Rev. Lett.* **50**, 1486 (1983); *Phys. Rev. B* **31**, 1396 (1985).
- <sup>33</sup>R. M. Bradley, P. N. Strenski, and J.-M. Debierre, *Phys. Rev. B* **44**, 76 (1991).
- <sup>34</sup>J. F. Gouyet, *Physica A* **168**, 581 (1990).

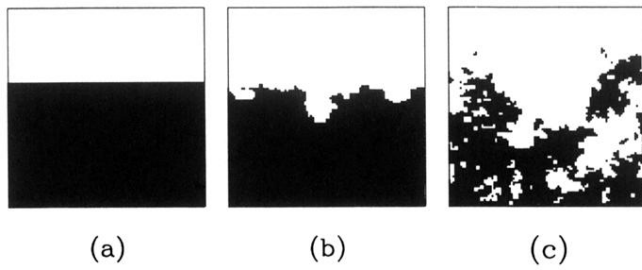


FIG. 2. Vertical cross sections of the domain structure for (a)  $\Delta = 2$ , (b)  $\Delta = 3$ , and (c)  $\Delta = 4.4$ . Dark regions represent flipped spins, and growth was started from a flat interface at the bottom of the cubic lattice.